

Modeling Correlation Degree between Two Adjacent Signalized Intersections for Dynamic Subarea Partition

Yiming Bie¹, Dianhai Wang², Xiaobo Qu³

¹ Lecturer, post-doctoral, School of Transportation Science and Engineering, Harbin Institute of Technology, Harbin, Heilongjiang 150091, China. E-mail: yimingbie@126.com

² Professor, Department of Civil Engineering and Architecture, Zijingang Campus, Zhejiang University, Hangzhou 310058, China (corresponding author). E-mail: wangdianhai@sohu.com

³ Lecturer, Griffith School of Engineering, Gold Coast campus, Griffith University, QLD 4222, Australia. E-mail: antielude@gmail.com

Abstract: Correlation degree between adjacent signalized intersections is considered as the most important component in subarea partition algorithm. In this study, contributing factors for subarea partition are selected by taking into consideration the differences with respect to cycle lengths, link length and path flow between upstream and downstream coordinated phases. Their impacts on performance index of subarea partition are further studied using numerical experiments. The paper then proceeds to propose a correlation degree index (CI) as an alternative for the performance index in order to reduce the computational complexity. The relationship between CI and the contributing factors is established to predict the correlation degree. Finally, the model is validated using field survey data.

1. Introduction

Subarea partition is of great importance to traffic control system since the selection of signal timing method for each intersection is determined by the partition results. Within a given subarea, the cycle lengths and phasing plans for different intersections are designed in such a way as to facilitate progressive movements and thereby reduce number of stops and delay [1].

The objective of subarea partition is to identify whether control performance can be improved when signal coordination is implemented to adjacent intersections. If the performance is improved, the adjacent intersections can be partitioned into one subarea. Therefore, a straightforward method for subarea partition is to calculate and compare the control performances with respect to signal coordination and isolated control algorithms. However, this method is not easy to be implemented in practice, although it is uncomplicated. This is because it would be time-consuming to iteratively estimate the performances of hundreds of adjacent intersections. Thus, an effective alternative is to propose an index reflecting the changes of control performances indirectly, which is called correlation degree index (CI) in this paper. As an appropriate alternative to control performances with a simpler form, it should accurately predict the change of control performances. Accordingly, the development of a model for CI is of great significance to subarea partition.

However, from the literature, little has been done on subarea partition, although it is essential in reality. The concept of subarea partition was first raised by Walinchus [2]. In his study, the contributing factors of subarea partition include the locations of significant changes in traffic flow characteristics (e.g. freeway access points from service roads, major arterials changed into urban grids, etc.). His study provided the fundamental basis for further study in subarea partition. Yagoda [3] concluded that the degree of coupling requirement was directly proportional to traffic volume

1 (V) and inversely proportional to link length (L) between two adjacent intersections. Thus, a
2 coupling index (I) is defined as $I = V/L$. Greater index indicates more desirable to have the two
3 intersections coupled. Although the model is theoretically sound, it lacks of reflecting the complex
4 changes in traffic pattern between two adjacent intersections. Chang [4] brought in the concept of
5 interconnection desirability index by considering both flow pattern and platoon dispersion
6 characteristic. If the value of the index was greater than 0.35, two intersections should be grouped.
7 Bie et al. [5] demonstrated that the index could not vary quickly as the traffic state change. Lin and
8 Tsao [1] selected congestion index of intersection, critical block length, and continuation of traffic
9 movement as factors that may affect the performance of subarea partition. Mathematical equations
10 were established to quantify these factors. However, the authors did not establish the relationship
11 between control performance and the contributing factors. Lin and Huang [6] developed a linear
12 model for determining coordination of two adjacent signalized intersections from the view of
13 block length. The model consisted of the dependent variable critical block length, and the
14 independent variables original platoon size and platoon completeness ratio. A deficiency of the
15 study is that block length itself only depicts partial picture of factors that affects subarea partition.
16 Bie et al [5] chose not only cycle length but also platoon length as contributing factors. An
17 integrated correlation model was developed to quantify the correlation degree between two
18 adjacent intersections. However, the determinations of weighted coefficients in the model and
19 threshold value were dependent on experiences and lack of theoretical basis. Synchro [7] is
20 perhaps the only software that has a feature of subarea partition application. The software
21 calculates an empirical coordinatability factor based on several variables such as distance, travel
22 time, and traffic volume. The coordinatability factor provides indications whether an intersection

1 should be coordinated with other signals in the system. For example, a coordinatability factor of
2 100 means the signal should be coordinated with other signals, while a factor below 20 would
3 suggests that the signal operates better independently.

4 Even in modern traffic adaptive control systems, studies pertaining to correlation model and
5 subarea partition are also not many. In SCOOT [8], the network was partitioned on the basis of
6 experiences of engineers and the form of subarea was fixed with traffic demand variation. In
7 SCATS, a simple index of integration or disjunction of subareas is proposed based on the
8 differences between cycle lengths [9]. In RHODES, it was expected that nine intersections could
9 be controlled as the reasonable size of a subarea without enormous computational effort [10].

10 As for real-time traffic control systems, an appropriate correlation degree index should reflect
11 dynamic characters of traffic flow and interactions among adjacent intersections. The objective of
12 this study is to propose an approach that is able to estimate a dynamic correlation degree index
13 between two adjacent intersections for subareas partition. Contributing factors are taken into
14 account in the proposed correlation degree model. This study could be the groundwork for
15 correlation degree index among multiple intersections.

16 **2. Development of Correlation Degree Model**

17 **2.1 Contributing factors of correlation degree**

18 The factors that affect the improvement of signal coordination would also be those affect subarea
19 partition. In this section, the factors that should be included in subarea partition are described.

20 These factors are the difference of cycle lengths between two adjacent intersections, link length
21 and path flow between upstream and downstream coordinated phases.

22 **(1) Difference of cycle lengths between two adjacent intersections**

1 Intersections in a subarea usually execute common cycle length (CCL) as to obtain maximum
2 green wave bandwidth and maintain optimal offsets. For a subarea with two intersections, the
3 intersection that operates maximum cycle length (MCL) is determined as seed intersection and its
4 cycle length is set as CCL. However, vehicle delay of the other intersection would increase
5 because CCL may be larger than its optimal cycle length (OCL). The increase range is directly
6 proportional to the difference between CCL and OCL. When the difference is large enough, the
7 increased vehicle delay may be larger than the delay reduced by signal coordination.

8 **(2) Link length between two adjacent intersections**

9 Signal coordination can reduce vehicle delay by providing green time for coming traffic platoon.
10 A compact platoon proves to be effective in improving coordination benefits because more
11 vehicles may pass the stop line in green time. According to Robertson's platoon dispersion model
12 [11], original platoon departs from upstream stop line would disperse to some extent and the
13 dispersion level is directly proportional to link length. Accordingly, a long link would have a
14 negative impact on arterial progression.

15 **(3) Path flow between upstream and downstream coordinated phases**

16 When a platoon that departs from upstream coordinated phase travels to downstream
17 intersection, some vehicles in the platoon may turn to uncoordinated downstream phases.
18 Therefore, the path flow that between the upstream and downstream coordinated phases may be
19 less than the original flow departs from upstream coordinated phase. Larger path flow indicates
20 more vehicles travel between the two phases and more vehicle delays have the opportunity to be
21 reduced by signal coordination. Thus, the correlation degree is directly proportional to the path
22 flow.

2.2 Performance index

The performance index of subarea partition should change as the traffic states of intersections vary. For example, the purpose of partitioning unsaturated adjacent intersections is to reduce vehicle delay. However, for saturated adjacent intersections, the purpose is to maximize capacity or minimize queue length. In this paper, we only study the unsaturated adjacent intersections, thus vehicle delay is selected as the performance index.

Let us take two adjacent signalized intersection i and j for example. Their total vehicle delay per cycle is denoted as D_i and D_j when they running isolated control algorithms. D_i or D_j can be obtained by the delay function in HCM 2000 [12]. If the two intersections are grouped into one subarea, they would run signal coordination algorithm. In such situation, total vehicle delay per cycle is denoted as \hat{D}_i and \hat{D}_j . The improved performance of grouping i and j into one subarea can be calculated by (1).

$$PI = D - \hat{D} \\ = (D_i \frac{3600}{C_i} + D_j \frac{3600}{C_j}) - (\hat{D}_i + \hat{D}_j) \frac{3600}{\max(C_i, C_j)} \quad (1)$$

In (1), C_i is the OCL of i when running isolated control algorithms. $\max(C_i, C_j)$ is the CCL when running signal coordination. D is the total vehicle delay per hour with respect to isolated control algorithms and \hat{D} is the total vehicle delay per hour with respect to signal coordination. All evaluation indices are unified as total vehicle delay per hour (the unit of PI is s/h). Because the OCL of non-seed intersection may be smaller than the CCL. Thus, the number of arrival vehicles each cycle may also be smaller than that when operating different timing methods.

PI is larger than 0 indicates that signal coordination can obtain better performance than isolated control, therefore, intersection i and j can be partitioned into one subarea. Otherwise i and j must be partitioned into different subareas.

2.3 Quantification the impact of difference of cycle lengths on CI

The best way to analyze the impact of difference of cycle lengths on PI is to develop a function between them based on theoretical derivation, and then calculate the variable quantity of PI

1 resulting from the unit change in difference of cycle lengths. However, \hat{D} in (1) is difficult to be
 2 obtained due to complex characters of vehicle movements on consecutive intersections. Thus,
 3 numerical experiments are adopted in this paper.

4 Also take intersection i and j for example, link length L equals 400 m and average vehicle speed
 5 is 12 m/s. j is the seed intersection and i is the non seed intersection. When the intersections run
 6 signal coordination, the OCL of j is set as the CCL. The difference between OCL of i and CCL
 7 increases with a step of 5 s while link length and path flow are fixed. Table 1 shows the output
 8 results of two experimental scenarios. In the two scenarios, CCL equals 125 s and 110 s
 9 respectively. In Table 1, the improved range equals the proportion of PI to D . The larger the range
 10 is, the better the signal coordination benefits are.

11 Take scenario 1 as an example, when OCL of i equals 90 s, the difference between cycle lengths
 12 is 35 s and PI equals 20,044 s. The improved range is only 5.7%. However, when OCL of i
 13 increases to 125 s, the improved range is 17.24%. The difference is negatively correlated to the
 14 improved range and the similar trend is obtainable in other scenarios. The results indicate that the
 15 difference between cycle lengths has a substantial impact on PI.

16 Table 1. Output results of the two experimental scenarios

Scenario	OCL of i/s	OCL of j/s	$D/s \cdot h^{-1}$	PI/ $s \cdot h^{-1}$	Improved range
1	90	125	351576	20044	5.70%
	95		358915	25438	7.09%
	100		371277	34919	9.41%
	105		378642	40453	10.68%
	110		390619	50311	12.88%
	115		399471	57848	14.48%
	120		408876	65726	16.07%
	125		416925	71878	17.24%
2	90	110	322504	22407	6.95%
	95		331007	28399	8.58%
	100		342658	37425	10.92%
	105		351739	44573	12.67%
	110		360691	51658	14.32%

17

1 The data shown in Table 1 can also be interpreted as follows. When the difference equals 0,
 2 signal coordination can obtain maximum benefits, which means the correlation between the two
 3 intersections is maximal and correlation degree index (CI) is 1.0. However, when the difference
 4 equals 35 s, the proportion of the improved range out of that when the difference equals 0 is only
 5 33%, that is, CI decreases to 0.33.

6 As can be seen from Table 1, CI is affected by not only the difference of cycle lengths, but also
 7 the CCL. Thus, the difference of cycle lengths is normalized as follows.

$$8 \quad C_D = \frac{C_j - C_i}{C_j} \quad (2)$$

9 For the 2 scenarios, the scatter diagrams between CI and normalized difference of cycle lengths
 10 C_D are shown in Fig.1.

11 There is a strong linear relationship between CI and C_D , and a linear function can be used to fit
 12 their relationship. The fitting formulas for the two subfigures are shown as follows.

$$13 \quad CI = \begin{cases} -2.471C_D + 1.024 & R^2 = 0.995 \\ -2.894C_D + 1.009 & R^2 = 0.996 \end{cases} \quad (3)$$

14 Linear functions can fit the scatter diagrams very well as indicated by the high R-square values.
 15 However, problem is that the slopes of the two lines are different from each other. This indicates
 16 that in different scenarios, C_D would pay different impacts on CI. Therefore, a universal function
 17 is needed to depict the relationship between the two variables, and to make the slope vary as traffic
 18 state changes. The linear functions in (3) can be replaced by the following format:

$$19 \quad CI(C_D) = \alpha_1 \cdot C_D + b_1 \quad (4)$$

20 Where α_1 is the slope of the function, b_1 is the intercept.

21 In reality, b_1 should equal to 1.0. However, due to fitting errors of (3), there exist marginal
 22 differences between the intercepts and 1.0. In this study, the differences are neglected and the
 23 value of b_1 is set as 1.0 directly. Therefore, only α_1 is needed to be fit in (4).

24 α_1 represents the variable quantity of CI resulting from the unit change in C_D . It may be affected

1 by many factors, such as green split and volume to capacity ratio (v/c) of coordinated phases, v/c
 2 of uncoordinated phases, total v/c , CCL and intersection saturation degree x . To study the impacts
 3 of these factors on α_1 , a multivariate regression can be adopted. The factors are introduced into the
 4 fitting function firstly and then eliminating the variables stepwise according to the correlation until
 5 the given precision is achieved. Then residual variables in the function are those pay significant
 6 impacts on α_1 . The amount of data in Table 1 is not enough for the regression model. Accordingly,
 7 another 6 experiments are carried out and total 8 groups of data are obtainable. The regression
 8 function is shown in (5).

$$9 \quad \alpha_1 = 14.916 - 53.963 \cdot x + 4.831 \cdot \lambda_c + 36.281 \cdot Y, \quad R^2 = 0.92 \quad (5)$$

10 In the function, λ_c is the green split of coordinated phase and Y is total v/c . Only three variables
 11 are left and other variables are excluded. F test is carried out to identify whether the real value and
 12 fitted value of α_1 differ significantly under a given significance level of 0.05, and the results of the
 13 test is acceptable.

14 **2.4 Quantification the impact of link length on CI**

15 Numerical experiments are conducted to establish the relationship between link length L and CI .
 16 During the experiments, L is increased from 200 m to 1500 m with a step of 50 m while cycle
 17 lengths of the two intersections and the path flow between coordinated phases is fixed in each
 18 scenario. Besides, cycle lengths of intersection i and j are same to each other. Fig.2 shows the
 19 output results of two typical scenarios. In scenario one and scenario 2, the cycle lengths of i and j
 20 equal 90 s.

21 In Fig.2, L and PI have a curvilinear relationship and the two curve shapes are similar to each
 22 other. As the value of L increases, the value of PI increases up to a maximum, which is attained at
 23 L equals about $0.5C_jV$. As L increases further, PI decreases and reaches a minimum value at L
 24 equals about $0.75C_jV$. The cycle is repeated along the increase of L with a step size of $0.5C_jV$
 25 meters. Difference is that the values of maximum and minimum decrease step by step. This
 26 changing tendency is significantly different with our straightforward view, because traditionally

we think PI would decrease linearly with the increase of L. However, the straightforward view is based on one-directional signal coordination and in this study we mainly focus on dual-directional signal coordination of the two adjacent intersections. When L equals the integral multiple of $0.5C_jV$, dual-directional interactive coordination is the best and thus traffic control can obtain maximum benefits. When L equals odd times of $0.25C_jV$, dual-directional coordination produces worst benefits and thus PI is minimal.

In numerical experiments L is increased with a step of 50 m and the integer times of $0.25C_jV$ do not equal the integer times of 50. Thus, to obtain the exact curvilinear relationship between L and PI, the values of PI corresponding to integer times of $0.25C_jV$ are supplemented.

When PI reach maximum value at L equals $0.5C_jV$, partition the two intersections into one subarea can obtain maximum control benefits, in such case CI equals 1.0. In other cases, CI equals the proportion of PI out of the maximum value of PI. L is normalized as follows:

$$L_c = \frac{L}{L_{\max}} \quad (5)$$

Where L_c is the normalized link length.

L_{\max} is recommended as 1500 m in this study because signal coordination is not suitable when L is larger than 1500 m according to engineering experiences. The relationship between CI and L_c is similar to that in Fig.2. Thus, the scatter diagrams between them are not displayed.

It is found that piecewise linear function may be suitable to fit the curve after detailed analysis. Moreover, the differences of two adjacent minimal values of CI are nearly a constant, and the differences between maximal values of CI and its left minimal values are also nearly a constant. For scenario 1 and 2, the extreme values of CI corresponding to integer times of $0.25C_jV$ are shown in Table 2.

Table 2. Values of CI corresponding to the extreme points

Scenario	First minimum	First maximum	Second minimum	Second maximum	Third minimum
1	0.663	1	0.533	0.858	0.4
2	0.674	1	0.527	0.816	0.372

1 In scenario 1, the difference between the first maximum and minimum equals 0.337. The
 2 difference between the second maximum and minimum equals 0.325. The two numbers are very
 3 close. Besides, the difference between the first minimum and second minimum equals 0.130. The
 4 difference between the second minimum and third minimum equals 0.133. They are also very
 5 close. In scenario 2 the same phenomenon is obtainable. The extreme points of the L_c -CI curve are
 6 labeled and shown in Fig.3 to model conveniently.

7 In numerical experiments, L ranges from 200 to 1500. However, L should be larger than 0. Thus,
 8 in Fig.3 the section that L belongs to the interval [0, 200] is supplemented to make the curve intact.
 9 But the values of CI corresponding to that interval do not have practical meanings. Because when
 10 L is smaller than 200 m, the objective of signal control should be to minimize queue length or
 11 avoid queue spillovers, other than reduce vehicle delay. On the basis of the changing tendency of
 12 CI, $y(0)$ should be larger than 1.0. But it does not have practical meaning. Therefore, it is set as
 13 1.0 to model conveniently.

14 To fit the curve in Fig.3 using piecewise linear function, the values of $y(1)$ and $y(3)$ are needed.
 15 The difference between $y(2)$ and $y(1)$ represents the reduction range of CI when the link length
 16 decreases from $0.5C_jV$ to $0.25C_jV$. Similarly, the difference between $y(2)$ and $y(3)$ represents the
 17 reduction range of CI when the link length increases from $0.5C_jV$ to $0.75C_jV$. The reduction
 18 ranges are affected by many factors, such as CCL, green split and v/c of coordinated phase, v/c of
 19 uncoordinated phases, total v/c and saturation degree x . The multivariate regression method shown
 20 in section 3.2 is also adopted here to distinguish whether the above factors pay significant impacts
 21 on $y(1)$ and $y(3)$. Total 10 groups of data are used in the regression.

22 The regression functions are shown in (6). In the two functions, only x , y_c and Y are left and
 23 other variables are excluded. y_c is the v/c ratio of coordinated phase.

$$24 \begin{cases} y(1) = 0.381 + 0.992 \cdot x - 0.87 \cdot Y + 0.291 \cdot y_c & R^2 = 0.95 \\ y(3) = -2.716 + 11.682 \cdot x - 9.814 \cdot Y + 1.942 \cdot y_c & R^2 = 0.96 \end{cases} \quad (6)$$

25 Then $y(n)$ in the L_c -CI curve equals:

$$y(n) = \begin{cases} 1.0 & n = 0 \\ 0.381 + 0.992 \cdot x - 0.87 \cdot Y + 0.291 \cdot y_c & n = 1 \\ 1.0 & n = 2 \\ -2.716 + 11.682 \cdot x - 9.814 \cdot Y + 1.942 \cdot y_c & n = 3 \\ y(n-1) + y(n-2) - y(n-3) & n \geq 4 \text{ \& even integer} \\ y(n-2) + y(n-4) - y(n-2) & n \geq 4 \text{ \& odd integer} \end{cases} \quad (7)$$

The n th one in the sets of lines can be fitted by (8).

$$CI_n(L_c) = \alpha_2 \cdot L_c + b_2$$

$$\begin{cases} \alpha_2 = \frac{y_n - y_{n-1}}{x_n - x_{n-1}} \\ b_2 = (y_{n-1} - \frac{y_n - y_{n-1}}{x_n - x_{n-1}} \cdot x_{n-1}) \end{cases} \quad (8)$$

Where α_2 is the slope of the line, b_2 is the intercept.

For scenario 1, the function between L_c and CI equals:

$$CI(L_c) = \begin{cases} -1.872 \cdot L_c + 1.0 & 0 \leq L_c \leq 0.18 \\ 1.872 \cdot L_c + 0.326 & 0.18 < L_c \leq 0.36 \\ -2.594 \cdot L_c + 1.934 & 0.36 < L_c \leq 0.54 \\ 1.871 \cdot L_c - 0.478 & 0.52 < L_c \leq 0.72 \\ -2.595 \cdot L_c + 2.738 & 0.72 < L_c \leq 0.90 \\ 1.871 \cdot L_c - 1.282 & 0.90 < L_c \leq 1.0 \end{cases} \quad (9)$$

The results of F test show that there is no significant difference between the real values and fitted values of CI. Thus, (9) can be used to depict the relationship between L_c and CI in scenario 1.

2.5 Quantification the impact of path flow on CI

Let q_s denotes the path flow and the maximum value of q_s (denoted as $q_{s \max}$) equals the maximum arrival flow of upstream coordinated phase. Because signal coordination is not suitable to be implemented to the intersection of which saturation degree is larger than X , thus $q_{s \max}$ is determined as the maximum historical traffic volume of upstream coordinated phase when its saturation degree is not larger than X . In this study, X is recommended as 0.90, because traffic jam may occur to one intersection when its saturation degree is larger than 0.90.

Also take intersection i and j for example. Two scenarios are tested firstly. Intersection i and j have the same cycle length and saturation degree. $q_{s \max}$ of the two scenarios are 640 pcu/h and

1 670 pcu/h respectively. The two directional path flows are the same. q_s is decreased from $q_{s\max}$ with
 2 a step of 5% $q_{s\max}$ while cycle length and link length are fixed.

3 Table 3 shows the output results. In the table P_q is the proportion of the difference between
 4 q_s and $q_{s\max}$ to $q_{s\max}$, which increases from 0 to 40%. D_u is the total vehicle delay per hour of
 5 uncoordinated phases. To keep the cycle length be fixed in each scenario, the reduced path flow is
 6 added to uncoordinated phases equally. Thus, the traffic flow and vehicle delay of uncoordinated
 7 phases would increase. D_c is the total vehicle delay per hour of coordinated phase. Because traffic
 8 volume of coordinated phase decreases gradually, D_c also decreases. P_{dc} is the decreased vehicle
 9 delay of coordinated phase compared with that when P_q equals 0. P_{du} is the increased vehicle delay
 10 of uncoordinated phases compared with that when P_q equals 0. PI_n is the negative performance
 11 index resulted by the decrease of q_s . P_n is the proportion of PI_n to the PI when P_q equals 0.

12 Table 3. Impact of difference between q_s and $q_{s\max}$ on control benefits

Scenario	P_q	D_u/s	D_c/s	P_{dc}/s	P_{du}/s	PI_n	P_n
1	0%	265103	77701	0	0	0	0.00%
	5%	271860	72611	5090	6757	1667	3.08%
	10%	276639	69391	8310	11536	3226	5.95%
	15%	283045	67884	9817	17942	8124	14.99%
	20%	287528	64228	13473	22425	8951	16.52%
	25%	297323	59695	18006	32220	14214	26.23%
	30%	299637	57025	20676	34534	13858	25.57%
	35%	305460	53310	24391	40357	15965	29.46%
	40%	309357	49541	28160	44254	16094	29.69%
2	0%	198840	59700	0	0	0	0.00%
	5%	202996	58878	613	4156	3543	5.95%
	10%	206948	57892	3032	8107	5075	8.52%
	15%	210717	56741	5926	11877	5950	9.99%
	20%	212268	56461	7176	13428	6253	10.49%
	25%	215648	54948	9405	16808	7403	12.43%
	30%	218853	53261	11658	20013	8354	14.02%
	35%	221884	51394	12925	23044	10118	16.98%
	40%	224744	49342	14916	25903	10988	18.44%

13
 14 In Table 3, the signal control between the two intersections can obtain maximum benefits
 15 when P_q equals 0. Therefore, CI equals 1.0. P_n indicates the degradation of PI with the increase
 16 of P_q . Take scenario 1 for example, P_n is 14.99% when P_q equals 15%. In such case the control

1 benefits equal 85.01% of the PI when P_q equals 0. That is, CI equals 0.8501. CI is the difference
 2 between 1.0 and $P_n \cdot P_q$ can be used as the normalized index of path flow. The scatter diagram
 3 between P_q and CI of the two scenarios are shown in Fig.4.

4 As can be seen from Fig.4, there is a strong linear relationship between P_q and CI. Linear
 5 function can be used to fit the scatter diagrams. The fitted functions are shown in (10). R-squares
 6 of the two functions are all larger than 0.94, which indicate that linear function can fit the
 7 relationship well.

$$8 \quad \begin{cases} CI(P_q) = -0.828 \cdot P_q + 0.9973 & R^2 = 0.95 \\ CI(P_q) = -0.401 \cdot P_q + 0.9726 & R^2 = 0.94 \end{cases} \quad (10)$$

9 Problem is that the slopes of the two functions are different. The slope is affected by many
 10 factors, such as CCL, green split and v/c of coordinated phase, v/c of uncoordinated phases, total
 11 v/c and saturation degree x . The multivariate regression method shown in section 3.2 is also
 12 adopted here to distinguish whether the above factors pay significant impacts on the slope. A
 13 universal function between P_q and CI is:

$$14 \quad CI(P_q) = \alpha_3 \cdot P_q + b_3 \quad (11)$$

15 Where α_3 is the slope, b_3 is the intercept.

16 In reality, b_3 equals 1.0. However, there are marginal differences between the intercepts in (10)
 17 and 1.0 because of fitting error. In this study, the differences are neglected and b_3 is set as 1.0.

18 Total 10 groups of data are used in the regression and the output results are as follows.

$$19 \quad e^{\alpha_3} = 5.946 - 2.664 \cdot \log(CCL) + 0.140 \cdot y_u - 0.049 \cdot \lambda_c, \quad R^2 = 0.93 \quad (12)$$

20 α_3 is affected by CCL, y_u and λ_c . (12) can be written as:

$$21 \quad \alpha_3 = \ln(5.946 - 2.664 \cdot \log(CCL) + 0.140 \cdot y_u - 0.049 \cdot \lambda_c) \quad (13)$$

22 In the above numerical experiments, the path flows of two directions are the same. However, in
 23 reality there may be difference between them. Other numerical experiments are also conducted
 24 and prove that P_q in (13) can be calculated by (14).

$$25 \quad P_q = \frac{(P_{q1} + P_{q2})}{2} \quad (14)$$

1 Where P_{q1}, P_{q2} are proportion differences of current path flow out of maximum historical path flow
 2 of the two directions.

3 **2.6 Integrated correlation degree model of two adjacent intersections**

4 In sections 2.3 to 2.5 the detailed relationships between contributing factors and CI are developed.
 5 To depict their joint impacts on CI, the following integrated correlation model is brought forward.

$$6 \quad \begin{aligned} CI &= 1 - [(1 - CI(C_D)) + (1 - CI(L_c)) + (1 - CI(P_q))] \\ &= CI(C_D) + CI(L_c) + CI(P_q) - 2 \end{aligned} \quad (15)$$

7 Where $CI(C_D)$, $CI(L_c)$ and $CI(P_q)$ can be obtained by (4), (8), and (11) respectively. In (15), the
 8 term $1 - CI(C_D)$ indicates the decrease of correlation degree because of the cycle length difference
 9 between the two adjacent intersections. The terms in the square brackets indicate the total decrease
 10 of correlation degree because of the three contributing factors.

11 PI is the improved network performance when signal coordination is implemented. When PI is
 12 larger than 0, the signal coordination can obtain better performance than isolated signal control. In
 13 such situation the two adjacent intersections can be partitioned into a same subarea, otherwise they
 14 must be partitioned into different subareas. In this paper CI is developed to simulate PI. When PI
 15 is larger than 0, CI is also larger than 0. Therefore, 0 is set as the threshold value of CI to
 16 distinguish whether the two adjacent intersections can be partitioned into a same subarea.

17 **3. Experiments and Validation**

18 An example is displayed to explain the correlation model established above. Field data are
 19 collected from two T type intersections in Fuzhou, the capital of Fujian Province, China. Sketches
 20 and phasing diagrams of the two intersections are shown in Fig.5. The two intersections carry out
 21 3 phases timing plans. Traffic volume of each lane is collected every 5 minutes and timing
 22 parameters are optimized and updated every 15 minutes.

23 To test whether CI can vary as the change of traffic state, two traffic scenarios are selected. One
 24 is based on the traffic flow operation from 10:45 to 11:00 in Dec 6, 2006. The other is based on

1 the traffic flow operation from 16:45 to 17:00 in Dec 6, 2006. Traffic volumes of the two scenarios
 2 are shown in Table 4.

3 Table 4. Arrival traffic volume of each lane

Scenario 1				Scenario 2			
Intersection A		Intersection B		Intersection A		Intersection B	
Lane	Volume (pcu·h ⁻¹)	Lane	Volume (pcu·h ⁻¹)	Lane	Volume (pcu·h ⁻¹)	Lane	Volume (pcu·h ⁻¹)
A1	268	B1	544	A1	355	B1	512
A2	616	B2	592	A2	572	B2	512
A3	608	B3	560	A3	584	B3	504
A4	626	B4	372	A4	572	B4	452
A5	516	B5	308	A5	440	B5	376
A6	524	B6	442	A6	448	B6	442
A7	508	B7	468	A7	420	B7	468
A8	308	B8	452	A8	388	B8	444
A9	276	B9	304	A9	284	B9	312
A10	356	B10	272	A10	336	B10	300

4 The differences between the two scenarios include two aspects. One is that the difference
 5 between cycle lengths of scenario 2 is larger than that of scenario 1. The other is that in afternoon
 6 more vehicles turn from Wuyi Road to Jintai Road and Fuxin Road, thus the path flow between
 7 the two coordinated phases is smaller than that of scenario 1. Table 5 shows the related parameters
 8 for the calculation of CI. From Table 5 we can find that the difference between the two cycle
 9 lengths increases from 10 s to 17 s.

10 Table 5. Parameters that related to the calculation of CI

Scenario 1			Scenario 2		
Parameters	Intersection A	Intersection B	Parameters	Intersection A	Intersection B
C_c/s	85	75	C_c/s	91	74
λ_c	0.45	0.43	λ_c	0.41	0.375
x	0.874	0.855	x	0.89	0.85
Y	0.78	0.75	Y	0.796	0.75
Y_c	0.39	0.37	Y_c	0.365	0.32
Y_u	0.39	0.38	Y_u	0.43	0.43

1 Then according to (15), the correlation degrees between A and B in the two scenarios are
 2 obtained and the results are shown in Table 6. In Scenario 1 and 2, CI equals 0.59 and 0.13
 3 respectively. Because two adjacent intersections can be partitioned into one subarea when CI is
 4 larger than 0, thus, in the two scenarios intersection A and B have the qualification to be combined.
 5 The CI in scenario 1 is larger than that in scenario 2 is because of the larger differences between
 6 cycle lengths and smaller path flow between the two coordinated phases in scenario 2.

7 Table 6. Calculating results of CI for the two scenarios

Parameters	α_1	α_2	α_3	$CI(C_D)$	$CI(L_c)$	$CI(P_q)$	CI
Scenario 1	-1.77	1.865	-0.576	0.79	0.91	0.88	0.59
Scenario 2	-2.25	1.77	-0.73	0.58	0.87	0.68	0.13

8 In scenario 1 CI is much larger than the threshold value 0. While in scenario 2, CI is near to 0.
 9 This indicates that in scenario 1 signal coordination can obtain much better performance than
 10 isolated control schemes. And in scenario 2, though the performance of signal coordination is
 11 better than isolated control schemes, the advantage is not significant.

12 To validate our conclusion, traffic data of the two scenarios are input into signal coordination
 13 algorithm and isolated control algorithm respectively. The control performances of signal
 14 coordination and isolated control of the two scenarios are produced, which are shown in Table 7.

15 Table 7. Comparisons between signal coordination and isolated control in the two scenarios

Scenario	1	2
Performance of Signal coordination / s	79692	81326
Performance of Isolated control / s	64128	76638
Improved range	19.5%	5.66%

16 From Table 7 we can find that in scenario 1, compared with isolated control, signal coordination
 17 can reduce total vehicle delay as much as 19.5%. However, in scenario 2 the proportion is only
 18 5.66%, which indicates that there is not obvious difference between the control performances of

1 signal coordination and isolated control. The results in Table 7 are accordance with that in Table 6.

2 Therefore, we can conclude that the correlation degree model developed in this study can reflect
3 the dynamic change of traffic state. Besides, CI is closely related to the change of PI, which
4 indicates that CI can be an alternative for PI. Accordingly, CI is worth trusting in subarea partition.

5 **4. Conclusions**

6 This paper developed a correlation degree model between two adjacent intersections by taking
7 consideration into three contributing factors, which are difference between cycle lengths, link
8 length and path flow between upstream and downstream coordinated phases. A case study was
9 displayed to explain the model and the results show that it is worth trusting in subarea partition.

10 This paper mainly focused on providing research thoughts for developing correlation degree
11 model between two intersections. Future research will be focused on developing correlation
12 degree model among multiple adjacent intersections and the subarea partition algorithm which can
13 partition intersections with high correlation degree into one subarea.

14 **ACKNOWLEDGEMENTS**

15 This study is supported by the National High Technology Research and Development Program
16 of China (Grant No. 2011AA110304).

17 We are grateful to Liang-Tay Lin and Shou-Min Tsao, their paper helps us find some usefully
18 related literatures and provides us meaningful research thought.

19 **REFERENCES**

- 20 [1] Lin L. T. and Tsao S. M.: 'A system approach on signal grouping for areawide control of computerized traffic
21 system', Proceedings of 79th Annual Meeting of the Transportation Research Board, Washington D. C., U. S.
22 A., January 2000, pp. 1-21

- 1 [2] Walinchus R.J.: 'Real-time network decomposition and subnetwork interfacing', Highway Research Record,
2 1971, 366, pp.20-28
- 3 [3] Yagoda N. H.: 'Subdivision of signal systems into control areas', Traffic Engineering, 1973, 43, (12), pp.42-45
- 4 [4] Chang, E. C. P.: 'Evaluation of interconnected arterial traffic signals', Transportation Planning Journal
5 Quarterly, 1986, 1, (15), pp.137-156
- 6 [5] Bie Y. M., Wang D. H., Wei Q., et al: 'Development of correlation degree model between adjacent signal
7 intersections for subarea partition', Proceedings of the 11th International Conference of Chinese Transportation
8 Professionals, Nanjing, China, August 2011, pp.1-11
- 9 [6] Lin L. T., and Huang H. J.: 'A linear model for determining coordination of two adjacent signalized
10 intersections', Journal of Modeling in Management, 2009, 4, (2), pp. 162-173
- 11 [7] Husch, D., and Albeck, J.: 'Synchro 6: Traffic signal software; user guide', 2003, Albany, Calif.
- 12 [8] Robertson, D. I.: 'Optimizing networks of traffic signals in real time-the SCOOT method', IEEE Transactions
13 on vehicular technology, 1991, 40, (1), pp.11-15
- 14 [9] Sims, A. G., and Dobinson K. W.: 'The Sydney Coordinated Adaptive Traffic (SCAT) system philosophy and
15 benefits', IEEE Transactions on Vehicular Technology, 1980, 29, (2), pp. 130-137
- 16 [10] Mirchandani P., and Head L.: 'RHODES: A real-time traffic signal control system: architecture, algorithms,
17 and analysis', Transportation Research Part C, 2001, 9, (6), pp. 415-132
- 18 [11] Robertson, D. I : 'TRANSYT A traffic network study tool-Report', No. 253, TRRL Laboratory, London,
19 U.K., 1969
- 20 [12] Transportation Research Board: 'Highway Capacity Manual', (Transportation Research Board, 2000)
- 21

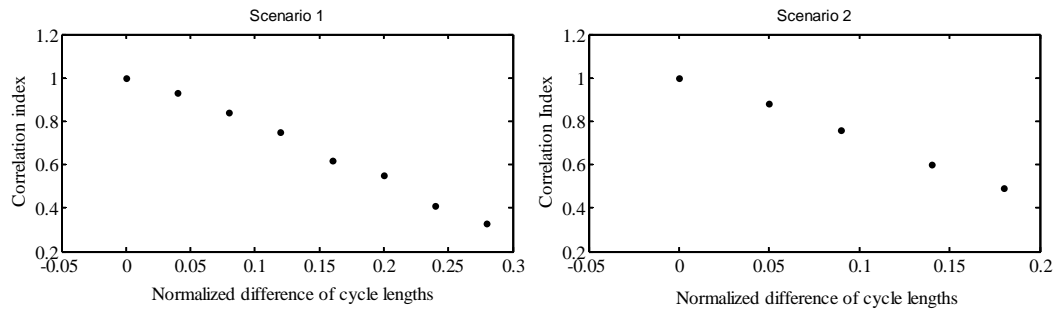


Fig.1 Scatter diagrams between CI and normalized difference of cycle lengths

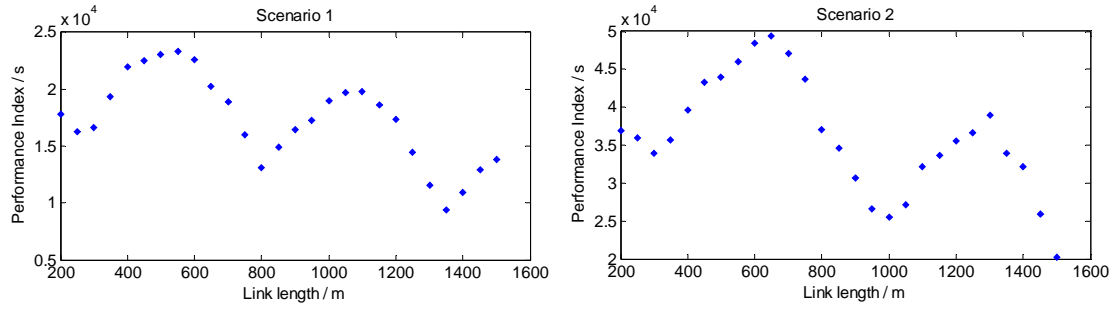


Fig.2 Scatter diagrams between L and PI of the two scenarios

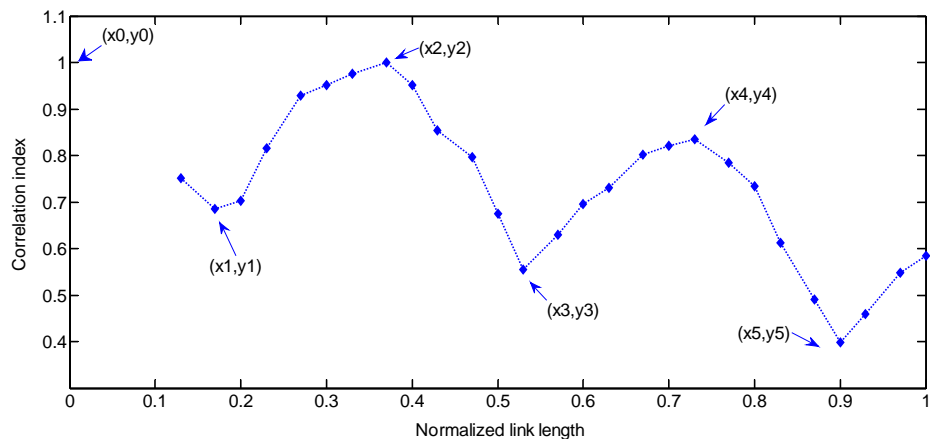


Fig.3 Scatter diagram between L_c and CI in scenario 1

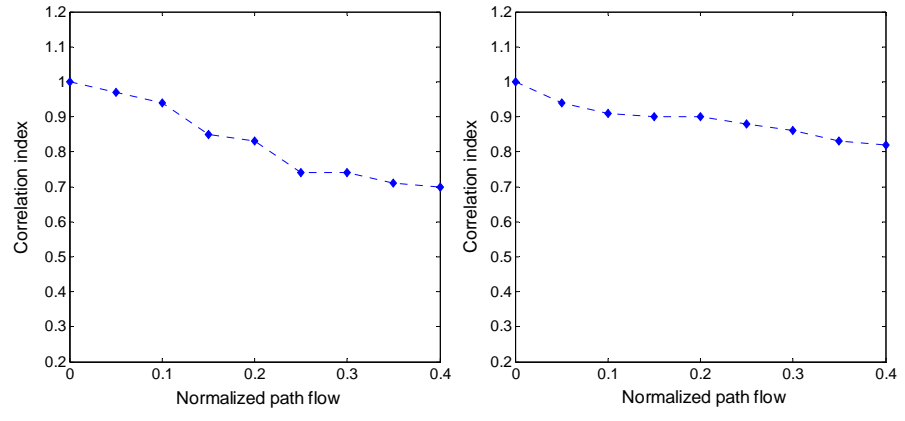


Fig.4 Scatter diagrams between normalized path flow and CI

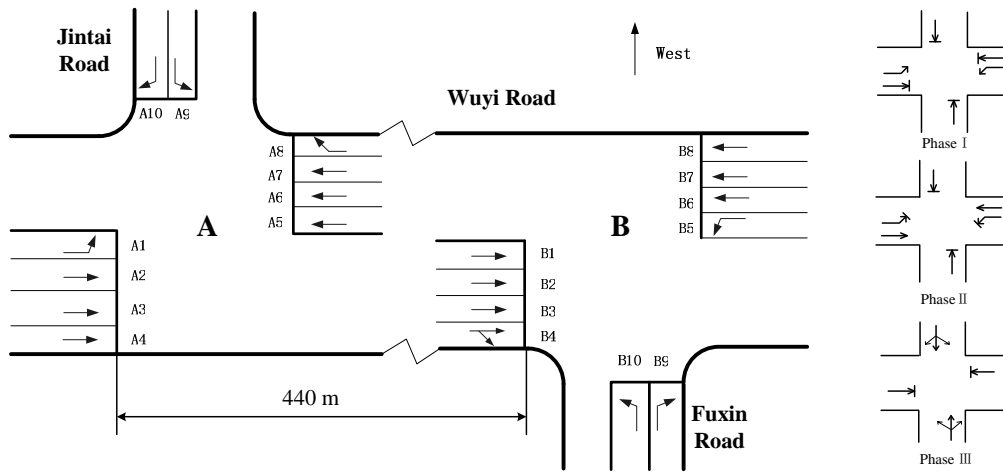


Fig.5 Sketch and phasing diagram of the two adjacent intersections